ACS APPLIED MATERIALS & INTERFACES

Research Article

www.acsami.org

Functionalized Carbon Quantum Dots with Dopamine for Tyrosinase Activity Monitoring and Inhibitor Screening: In Vitro and Intracellular Investigation

Lujing Chai,[†] Jin Zhou,[‡] Hui Feng,[†] Cong Tang,[†] Yuanyuan Huang,[†] and Zhaosheng Qian*[,†]

[†]College of Chemistry and Life Science, Zhejiang Normal University, Jinhua 321004, China

[‡]Beijing National laboratory for Molecular Sciences, Key Laboratory of Analytical Chemistry for Living Biosystems, Institute of Chemistry, Chinese Academy of Sciences, Bejing 100190, China

Supporting Information

ABSTRACT: Sensitive assay of tyrosinase (TYR) activity is in urgent demand for both fundamental research and practical application, but the exploration of functional materials with good biocompatibility for its activity evaluation at the intracellular level is still challenging until now. In this work, we develop a convenient and real-time assay with high sensitivity for TYR activity/level monitoring and its inhibitor screening based on biocompatible dopamine functionalized carbon quantum dots (Dopa-CQDs). Dopamine with redox property was functionalized on the surface of carbon quantum dots to construct a Dopa-CQDs conjugate with strong bluish green fluorescence. When the dopamine moiety in Dopa-CQDs conjugate was oxidized to a dopaquinone derivative under specific catalysis of TYR, an intraparticle photoinduced electron transfer (PET) process between CQDs and dopaquinone moiety took place, and then the fluorescence of the conjugate could be quenched simultaneously. Quantitative evaluation of TYR activity was established in terms of the relationship between fluorescence quenching efficiency and TYR activity. The assay covered a broad linear range of up to 800 U/L with a low detection limit of 7.0 U/L. Arbutin, a typical inhibitor of TYR, was chosen as an example to assess its function of inhibitor screening, and positive results were observed that fluorescence quenching extent of the probe was reduced in the presence of arbutin. It is also demonstrated that Dopa-CQD conjugate possesses excellent biocompatibility, and can sensitively monitor intracellular tyrosinase level in melanoma cells and intracellular pH changes in living cells, which provides great potential in application of TYR/pH-associated disease monitoring and medical diagnostics.

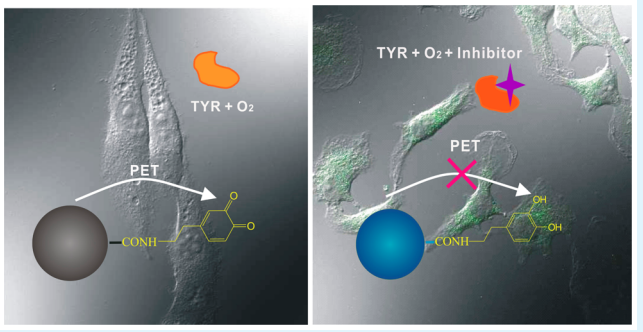

KEYWORDS: *tyrosinase, carbon quantum dots, fluorometric assay, inhibitor screening, intracellular imaging*

INTRODUCTION

Tyrosinase (TYR, EC 1.14.18.1) is a copper-containing polyphenol oxidase, which is widespread in microorganisms, animals, and plants. Two oxidation activities of tyrosinase have been identified: its monophenolase activity is catalytic hydroxylation of monophenol to o-diphenol, and its diphenolase activity is shown in catalytic oxidation of diphenol to o-quinones in the presence of molecular oxygen.[1] These specific activities of TYR can initiate the formation of melanin, which plays a vital protective role against skin photocarcinogenesis.[2] An abnormally elevated level of TYR can cause the production of melanin pigmentation that is considered as one of the serious esthetic problems in human beings, and thus, its inhibitors have been widely exploited as effective constituents for whitening product in cosmetic industry.[3] TYR activity/level is not only regarded as an important biomarker of melanoma cancer because of its overexpressed level in melanoma cancer cells,[4] but also acts as an autoantigen and serves as a marker for vitiligo.[5] In addition, TYR activity has been found to be one of the factors that influence the appearance, taste, and nutritional quality of vegetables and fruits.[6] Therefore, the development of a highly sensitive assay of tyrosinase activity is in urgent demand for both fundamental research and practical application in clinical diagnosis and cosmetic industry.

Traditional colorimetric assay for TYR activity depends on the characteristic absorbance of intermediates to achieve direct and quantitative tyrosinase detection.[7] Due to its unreliability and low sensitivity induced by instability of intermediate products, a variety of assays based on colorimetric,[8−10] electrochemical,[11] and fluorometric approaches[12−19] were developed. Among them, fluorometric assays are regarded as a more desirable approach because they generally possess higher sensitivity and can be used to detect TYR level in living cells in a real-time manner. The assays based on molecular probes often suffer from a tedious

Received: July 23, 2015
Accepted: October 6, 2015
Published: October 6, 2015

DOI: 10.1021/acsami.5b06711
ACS Appl. Mater. Interfaces 2015, 7, 23564−23574

synthesis procedure of the probe and instability to light,[12−15] while the assays based on inorganic semiconductor quantum dots (QDs) were concerned about the toxicity of used QDs.[16,17] Noble nanoclusters including silver and gold nanoclusters have also been used to assay TYR activity, but stabilizing agents have to be adopted due to their instability properties in aqueous solution, which makes these assays not easy to repeat.[18,19] Moreover, among the preceding assays, only two reports demonstrated the detection and imaging of TYR inside living cells with a molecular probe and QDs-Tyr conjugate, respectively,[14,17] but their instability to exposure light or potential cytotoxicity does not enable them as desirable choice for intracellular detection of TYR activity.

Carbon quantum dots (CQDs) with good stability and excellent biocompatibility, as a novel fluorescent carbon-based nanomaterial, have begun to play an increasingly important role in biosensor and bioimaging.[20−24] Because of its advantageous properties in biosensors, CQDs have been exploited to detect biological macromolecules including DNA,[25−27] miroRNA,[28] trypsin,[29] thrombin,[30] hyaluronidase,[31] and alkaline phosphatase.[32,33] In this study, we develop a convenient and real-time assay with high sensitivity for tyrosinase (TYR) activity/level monitoring and its inhibitor screening on the basis of dopamine functionalized carbon quantum dots (Dopa-CQDs) as the fluorescent probe. Carbon quantum dots with strong yellowish green fluorescence were used as the fluorophore, and dopamine with redox property was functionalized on the surface of carbon quantum dots to construct the Dopa-CQDs conjugate. Under specific catalytic oxidation of TYR in the presence of molecular oxygen, dopamine moiety in Dopa-CQDs could be transformed to o-dopaquinone derivative, which acts as an effective electron acceptor. Intraparticle photoinduced electron transfer (PET) inside the oxidative form of Dopa-CQDs could take place, where CQDs and dopaquinone moiety function as the electron donor and acceptor, respectively, and the fluorescence of the conjugate is quenched simultaneously due to this PET process. Thus, quantitative evaluation of TYR activity can be established in terms of the correlation between fluorescence signal readout and present TYR activity. However, when an inhibitor of TYR like arbutin was present, TYR activity could be heavily inhibited to lead to the increase in fluorescence as the rise in amount of the inhibitor because the inhibitor could reduce oxidation extent of Dopa-CQDs by TYR. Intracellular detection of TYR activity using the assay was also conducted successfully, which promises its bright prospect in practical application of TYR-associated disease monitoring and medical diagnostics.

EXPERIMENTAL SECTION

Materials and Reagents. Triple-distilled water was used throughout the experimental process. Activated carbon, arbutin, dopamine, $Na_2HPO_4{\cdot}12H_2O$, $NaH_2PO_4{\cdot}2H_2O$, EDC·HCl, and NHS were purchased from Aladdin Company (Shanghai, China). The tryosinase (TYR, EC 1.14.18.1) from mushroom, acetylcholinesterase (AChE, EC 3.1.1.7), alkaline phosphatase (ALP, EC 3.1.3.1) from bovine intestinal mucosa, acid phosphatase (ACP, EC 3.1.3.2) bovine serum albumin (BSA), immune globulin G (IgG), and gulcose oxidase (GOx, EC 1.1.3.4) from aspergilus niger were purchased from Sigma-Aldrich (Shanghai, China). 3-(4,5-Dimethylthiazol-2-yl)-2,5-diphenyltetrazolium bromide (MTT) was purchased from Serva Electrophoresis GmbH (Germany). Dulbecco's modified Eagle's media (DMEM), fetal bovine serum, penicillin (100 μg/mL), streptomycin (100 μg/mL), and phosphate buffered saline (PBS) solution were obtained from Invitrogen Corporation. 2-(4-(2-Hydroxyethyl)piperazin-1-yl)-ethanesulfonic acid (HEPES), 2-morpholinoethanesulfonic acid (MES), and nigericin were purchased from Alfa Aesar Company. PB buffer solution (pH 6.3) was prepared by mixing stock solution and adjusted to pH 6.3. All reagents were of analytical grade and used without any further purification.

Synthesis of Dopamine Functionalized CQDs (Dopa-CQDs) Conjugate. The detailed preparation procedure of CQDs was reported in our previous paper,[32,33] and thus herein was briefly described as follows: The mixture containing activated carbon powder (2.0 g), concentrated H_2SO_4 (180 mL), and HNO_3 (60 mL) were placed in an oil bath and heated at 80 °C for 5 h. The resultant mixture was cooled to room temperature and then diluted with triple-distilled water (800 mL), and further neutralized with sodium hydroxide. The final dark solution was dialyzed first using a dialysis bag (1 kDa) to remove small molecules and sodium salts, and then was treated using a dialysis bag (50 kDa) to remove large nonfluorescent materials.

To synthesize Dopa-CQDs conjugate, a known amount of CQDs solution (15 mL) was first put in a beaker, and then the pH of the solution was adjusted to 5−6. A certain amount of EDC·HCl (0.25 g) and NHS (0.25 g) were added into the CQDs solution under stirring to activate CQDs for 1 h. An excessive amount of dopamine (0.25 g) was added to the preceding solution and allowed for 24 h, where the pH was adjusted to about 7, and the resulting solution was bubbled with nitrogen to remove the dissolved oxygen. Finally, as-prepared solution was purified with microporous filter (0.22 μm) and a dialysis bag (1000 Da) to remove excessive dopamine, EDC, NHS, and possibly generated polydopamine.

Fluorescent Tyrosinase Assay. For optimization of incubation time for fluorescence quenching by tyrosinase, the fluorescence of Dopa-CQDs (PB, pH 6.3) was recorded in the presence of tyrosinase (7213.3 U/L) after different shaking times of 1.5, 3, 4.5, 6, 7.5, 9, 10.5, 12, and 13.5 min, respectively. Under the optimum incubation time, fluorescence quenching of Dopa-CQDs (PB, pH 6.3) was assessed with continuous addition of tyrosinase, where the activity of tyrosinase ranged from 23.2 to 14 355.2 U/L. The fluorescence spectra of the mixtures containing Dopa-CQDs (PB, pH 6.3) and different amounts of tyrosinase were monitored using fluorescence spectrometer at the optimal excitation wavelength of 315 nm.

Selectivity of the Tyrosinase (TYR) Assay. Under the optimal conditions, the selectivity of the assay toward TYR was evaluated. Seven biological species including bovine serum albumin (BSA), immune globulin G (IgG), acid phosphatase (ACP), alkaline phosphatase (ALP), DNA, and acetylcholinesterase (AChE) were selected to assess the selectivity of the sensing system toward TYR. Dopa-CQDs solution in PB buffer (pH 6.3) was first added into the cell, and its fluorescence was regarded as the control. Then, each of the following species including TYR, BSA, ACP, IgG, ALP, GOx, and DNA (2.454 g/L) was separately incubated with Dopa-CQDs solution (3.0 mL). All the mixtures incubated after 20 min were monitored using fluorescence spectrophotometer.

Inhibitor Screening. Arbutin as a model was used for inhibitor screening of TYR. To detect the inhibition effect, the mixtures containing TYR (80 μL, 230.8 U/mL) and different concentrations of arbutin ranging from 0.0 to 1666.7 μM were incubated for 10 min, and then were separately added into Dopa-CQDs solution (3.0 mL, pH 6.3). The fluorescence of the resulting mixture was recorded in a period of 24 min.

Cytotoxicity Test of Dopa-CQDs Conjugate. The cytotoxicity of Dopa-CQDs on human HeLa cells was evaluated by the standard MTT assay. Briefly, HeLa cells were seeded in 96-well U-bottom plates at a density of 7000 cells/well, and incubated with Dopa-CQDs at varying concentrations at 37 °C for 24 h. Then, the culture media were discarded, and 0.1 mL of the MTT solution (0.5 mg mL^{-1} in DMEM) was added to each well, followed by incubation at 37 °C for 4 h. The supernatant was abandoned, and 110 μL of DMSO was added to each well to dissolve the formed fromazan. After shaking the plates for 10 min, absorbance values of the wells were recorded with a microplate reader at 490 nm. The cell viability rate (VR) was calculated according to the following equation: $VR = A/A_0 \times 100\%$, where A is the absorbance of the experimental group (i.e., the cells were treated by Dopa-CQDs) and A_0 is the absorbance of the control group (i.e., the cells were untreated

DOI: 10.1021/acsami.5b06711
ACS Appl. Mater. Interfaces 2015, 7, 23564−23574

Scheme 1. Schematic Illustration of Detection Strategy for TYR Activity Based on Photoinduced Electron Transfer between CQDs and Dopaquinone Moiety

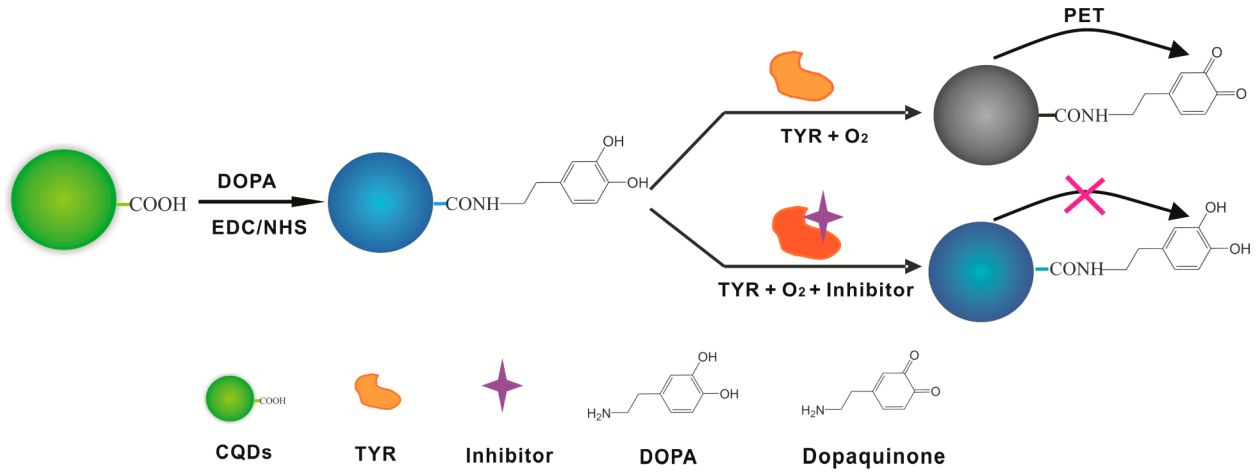

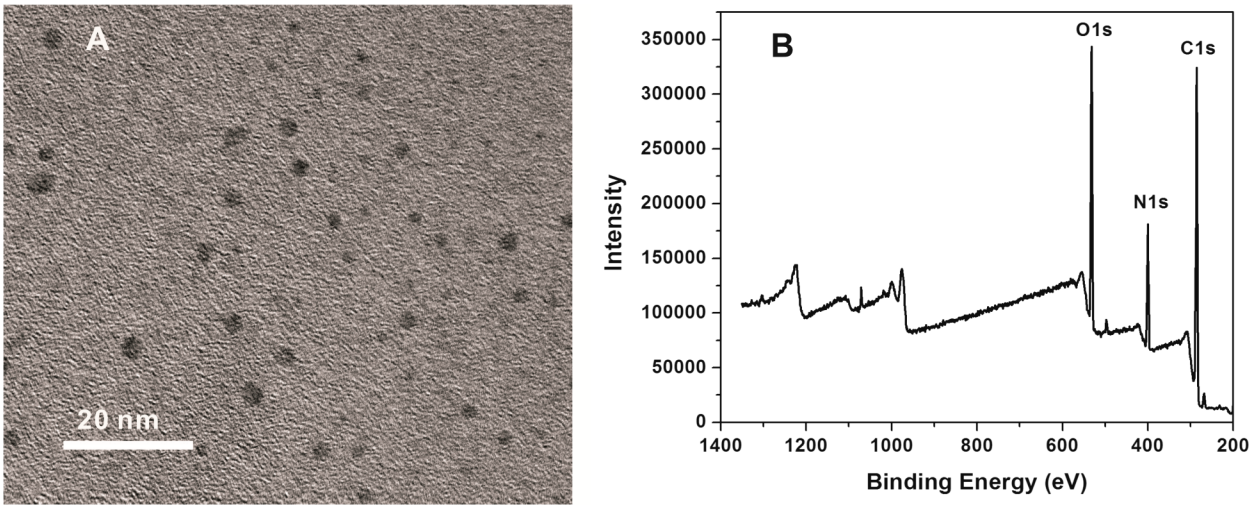

Figure 1. TEM image (A) and XPS wide spectrum (B) of Dopa-CQDs.

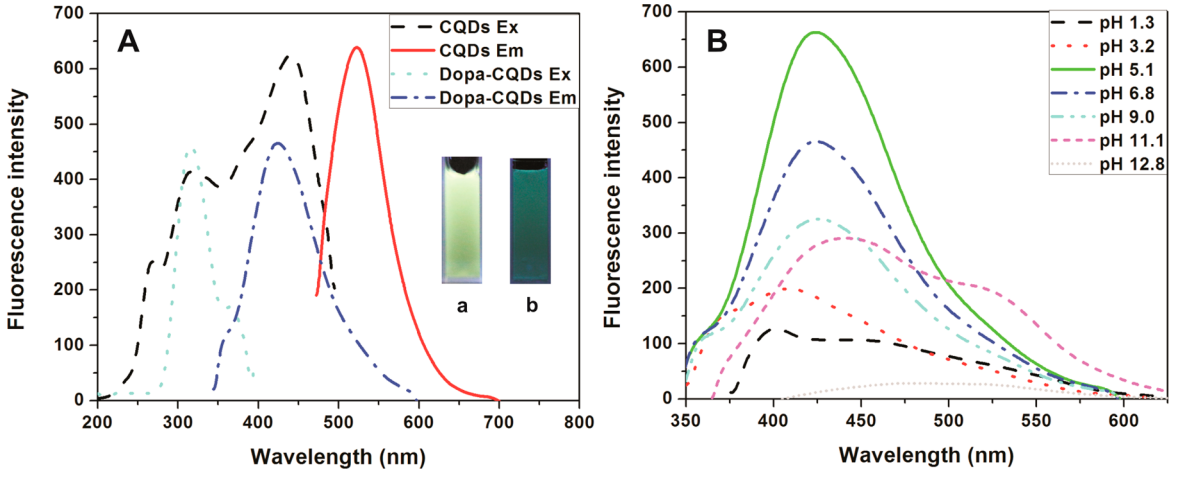

Figure 2. Fluorescence excitation and emission spectra of CQDs and Dopa-CQDs (A), and fluorescence spectra of Dopa-CQDs at variable pHs (B). Inset: Photographs of CQDs (a) and Dopa-CQDs (b) under UV lamp.

by Dopa-CQDs). The cell survival rate from the control group was considered to be 100%.

Cell Culture and Fluorescence Imaging. All cell lines (HeLa and B16 cells) used in this study were cultured in DMEM containing 10% (v/v) fetal bovine serum and 1% (v/v) penicillin−streptomycin at 37 °C in a 5% CO_2 incubator. For fluorescence imaging, the adherent cells grown on glass-bottom culture dishes (Mat Tek Co.) containing 1 mL of culture medium were first incubated with Dopa-CQDs (100 μg mL^{-1})

DOI: 10.1021/acsami.5b06711
ACS Appl. Mater. Interfaces 2015, 7, 23564−23574

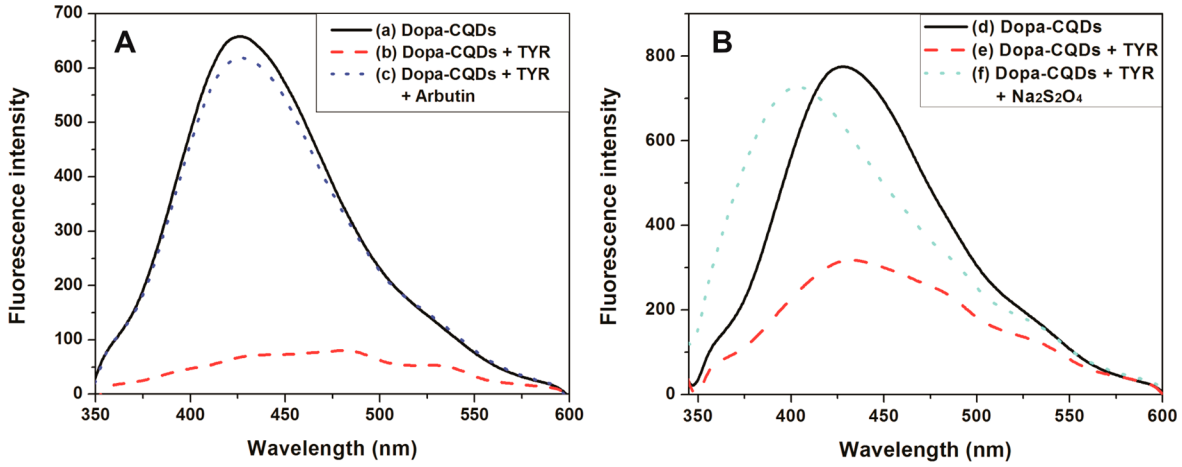

Figure 3. (A) Changes of fluorescence spectra of Dopa-CQDs in the presence of TYR and arbutin: (a) mere Dopa-CQDs, (b) in the presence of TYR (14355.2 U/L), (c) in the presence of TYR (14355.2 U/L) and arbutin (1666.7 μM). (B) The changes of fluorescence spectra of Dopa-CQDs in the presence of TYR and $Na_2S_2O_4$: (d) mere Dopa-CQDs, (e) in the presence of TYR (4616.8 U/L), (f) in the presence of TYR (4616.8 U/L) and $Na_2S_2O_4$ (333.3 μM).

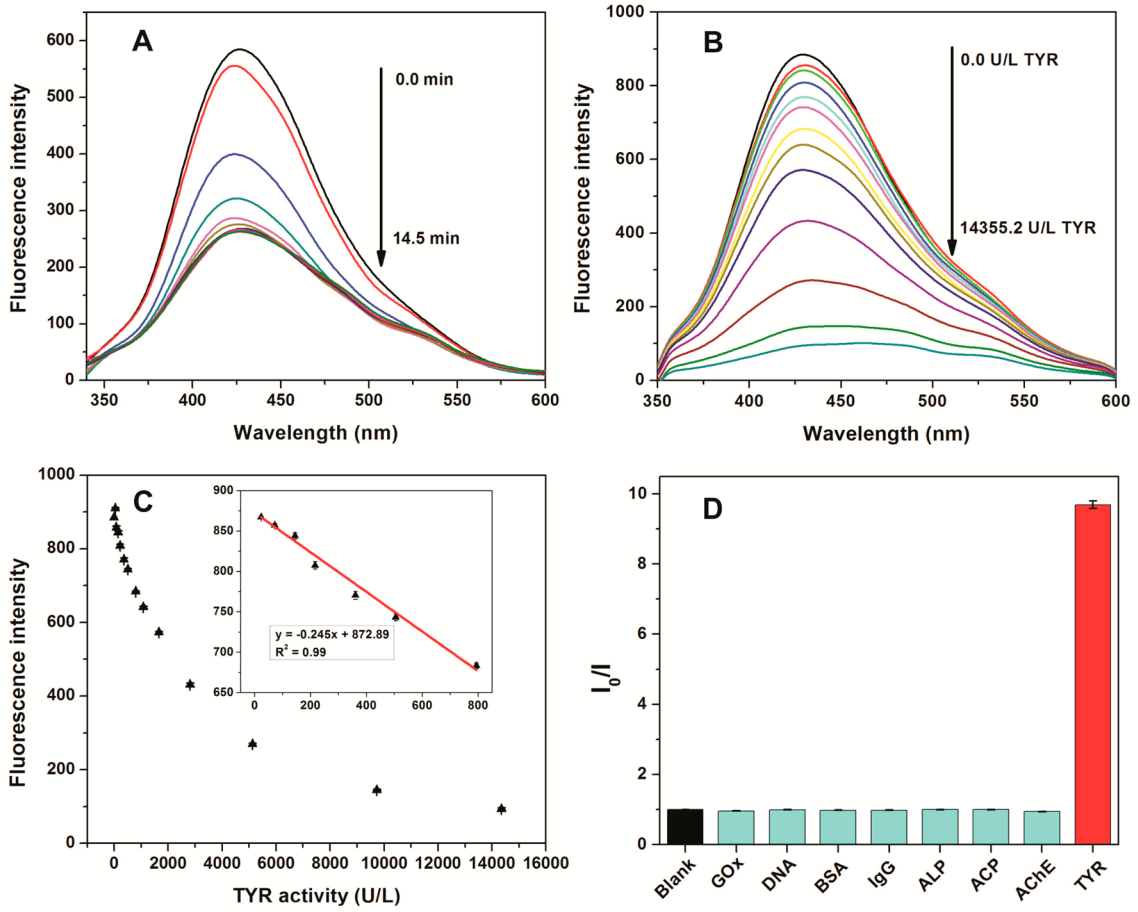

Figure 4. (A) Fluorescence spectra of Dopa-CQDs as a function of reaction time in the presence of tyrosinase (7213.3 U/L) at room temperature. (B) Fluorescence spectra of Dopa-CQDs as a function of TYR level after 20 min of incubation time. (C) Fluorescence intensity of Dopa-CQDs versus TYR activity ranging from 0.0 to 14355.2 U/L. Inset: The fitting curve and regression equation between fluorescence intensity and TYR activity over a linear range from 23.2 to 793.5 U/L. (D) Selectivity test of the assay toward TYR. I_0 and I represent the fluorescence intensity in the absence and presence of different composition including glucose oxidase (GOx), DNA, bovine serum albumin (BSA), immunoglobulin G (IgG), alkaline phosphatase (ALP), acid phosphatase (ACP), acetylcholinesterase (AChE), and tyrosinase (TYR). The concentration of each composition is 2.454 g/L, and TYR activity is 14 355.2 U/L.

for 5 h at 37 °C, and then washed with PBS solution (pH 7.4). Inhibitor effect was made by pretreatment of cells with arbutin, an inhibitor of TYR. Briefly, the B16 or HeLa cells were first incubated with arbutin (200 μM) for 30 min. After that, the cells were washed with PBS three

DOI: 10.1021/acsami.5b06711
ACS Appl. Mater. Interfaces 2015, 7, 23564−23574

times, and then incubated with Dopa-CQDs conjugate according to the above procedure.

For intracellular pH calibration, the Dopa-CQDs-loaded cells were incubated at 37 °C for 15 min in high K^+ buffer (30 mM NaCl, 120 mM KCl, 1 mM $CaCl_2$, 0.5 mM $MgSO_4$, 1 mM NaH_2PO_4, 5 mM glucose, 20 mM sodium acetate, 20 mM HEPES, and 20 mM MES) of various pH values in the presence of 10 μM nigericin.

Characterization Methods. Transmission electron microscopy (TEM) was conducted on a JEOL-Model 2100F instrument with an accelerating voltage of 200 kV. A Kratos Axis ULTRA X-ray photoelectron spectroscopy instrument was used for the X-ray photoelectron spectroscopy analyses. The UV−vis spectra were recorded on a PerkinElmer Lambda 950 spectrometer. The fluorescence spectra and time-resolved fluorescence decay tests were performed using a PerkinElmer Model LS 55 system, and an Edinburgh Instruments Model FLS920 fluorescence spectrophotometer. Fluorescence imaging experiments were performed on an FV 1000-IX81 confocal laser scanning microscope (Olympus, Japan) with FV5-LAMAR for excitation at 405 nm and a variable bandpass emission filter set to 425−525 nm through a 100 × 1.4 NA objective.

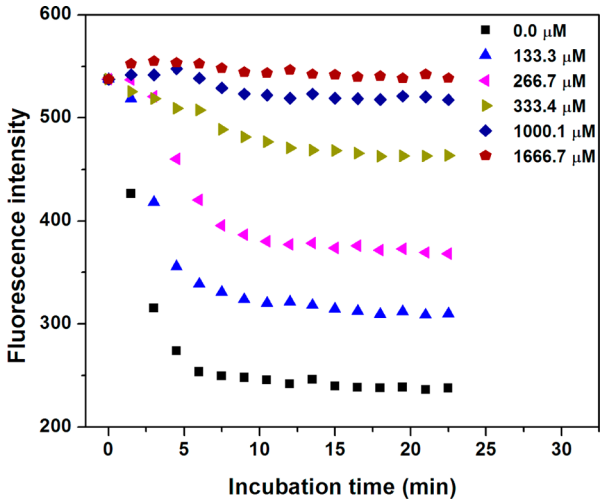

Figure 5. Changes of the fluorescence intensity of Dopa-CQDs conjugate reacting with tyrosinase (6155.7 U/L) at room temperature in the presence of different concentrations of arbutin (from bottom to top): 0, 133.3, 266.7, 333.4, 1000.1, and 1666.7 μM, respectively. The measurements were preformed in phosphate buffer solution.

RESULTS AND DISCUSSION

Principle of TYR Level Detection Based on Dopa-CQDs Conjugate. Carbon quantum dots from chemical oxidation of activated carbon powder possess many superiorities including excellent aqueous solubility, stable fluorescence emission, and abundant surface groups like carboxyl group, and thus are employed as the fluorophore in the conjugate. Dopamine, as one of the most important catecholamine neurotransmitters, shows a characteristic redox property and can be specifically oxidized by TYR to o-dopaquinone acting as an effective electron acceptor, which endows dopamine as the best choice to be the functional group. Scheme 1 shows the schematic illustration of detection strategy for TYR activity based on intrapaticle photoinduced electron transfer process between CQDs and o-dopaquinone moiety. Abundance in carboxyl group of as-prepared CQDs enables it to covalently bond with dopamine through EDC/NHS coupling reaction. Dopamine functionalized CQDs (Dopa-CQDs) conjugate was prepared in this way, and possesses bright bluish green fluorescence. Dopamine moiety in Dopa-CQDs conjugate can be transformed to o-dopaquinone under catalytic oxidation of TYR in the presence of molecular oxygen. Because the o-dopaquinone moiety in the oxidative form of the conjugate functions as an effective electron acceptor, intraparticle PET process can take place resulting in fluorescence quenching of the conjugate. The correlation between quenching efficiency and TYR activity can be used to establish a real-time assay for TYR activity. When an inhibitor of TYR is present in the assay solution, it would inhibit TYR activity and keep the conjugate in its reductive form. The following PET process can be blocked, and thus, the fluorescence would be retained. The inhibitor screening can be conducted in this way.

Synthesis and Characterization of Dopamine Functionalized CQDs (Dopa-CQDs) Conjugate. The CQDs were prepared by chemical oxidation of activated carbon according to our previous papers.[32,33] As shown in our previous report, as-prepared CQDs exhibit strong yellowish green fluorescence, and have a relative narrow size distribution ranging from 2 to 5 nm. Two major elements, oxygen (25.5 at. %) and carbon (74.5 at. %), can be identified from XPS spectra, and a vast number of oxygen-containing groups including carboxyl on the surface of CQDs are revealed. Dopamine functionalized CQDs were synthesized using dopamine and CQDs through condensation reaction. CQDs abundant in carboxyl group were first activated by EDC/NHS, and then mixed with an excessive amount of dopamine for 24 h at room temperature. As-prepared Dopa-CQDs conjugate was characterized by TEM, XPS, and fluorescence spectroscopy, respectively. As shown in Figure 1A, size distribution of Dopa-CQDs falls in the range 2−5 nm, which is consistent with that of mere CQDs because the small dopamine functionalized on the surface of CQDs could not apparently change the size of CQDs. The XPS spectrum in Figure 1B clearly illustrated that Dopa-CQDs are composed of carbon, oxygen, and nitrogen, and nitrogen is present in the form of amide (399.7 eV), indicating that dopamine was covalently linked on the surface of CQDs through the amide moiety. Element analysis displayed that the contents of carbon, oxygen, and nitrogen in Dopa-CQDs are 65.9 at. %, 19.9 at. %, and 14.2 at. %, respectively, and 14.2% of nitrogen originated from functionalized dopamine. Bright bluish green fluorescence of Dopa-CQDs solution can be observed under UV lamp, and its fluorescence is apparently blue-shifted in comparison with yellowish green fluorescence of mere CQDs. This point is further verified by their fluorescence spectra as shown in Figure 2A. Original CQDs fluoresce at the optimal peak of 525 nm when the excitation wavelength of 440 nm was used, while Dopa-CQDs conjugate exhibits an emission band centered at 425 nm when excited at 315 nm. It was found (Figure S1, Supporting Information) that the emission peak of Dopa-CQDs remained constant at the excitation wavelengths ranging from 300 to 340 nm, but was shifted along with excitation wavelength when its excitation wavelength was over 340 nm. The fluorescence quantum yield of Dopa-CQDs was determined to be 1% using sulfate quinine as the reference standard. Time-resolved fluorescence decay curve of Dopa-CQDs conjugate was displayed in Figure S2, and its lifetime was calculated as 2.80 ns on the basis of the decay curve, which is much shorter than that of CQDs (6.2 ns).[32] Substantial differences in emission peak and lifetime between Dopa-CQDs and original CQDs provide further proof for successful preparation of Dopa-CQDs.

DOI: 10.1021/acsami.5b06711
ACS Appl. Mater. Interfaces 2015, 7, 23564−23574

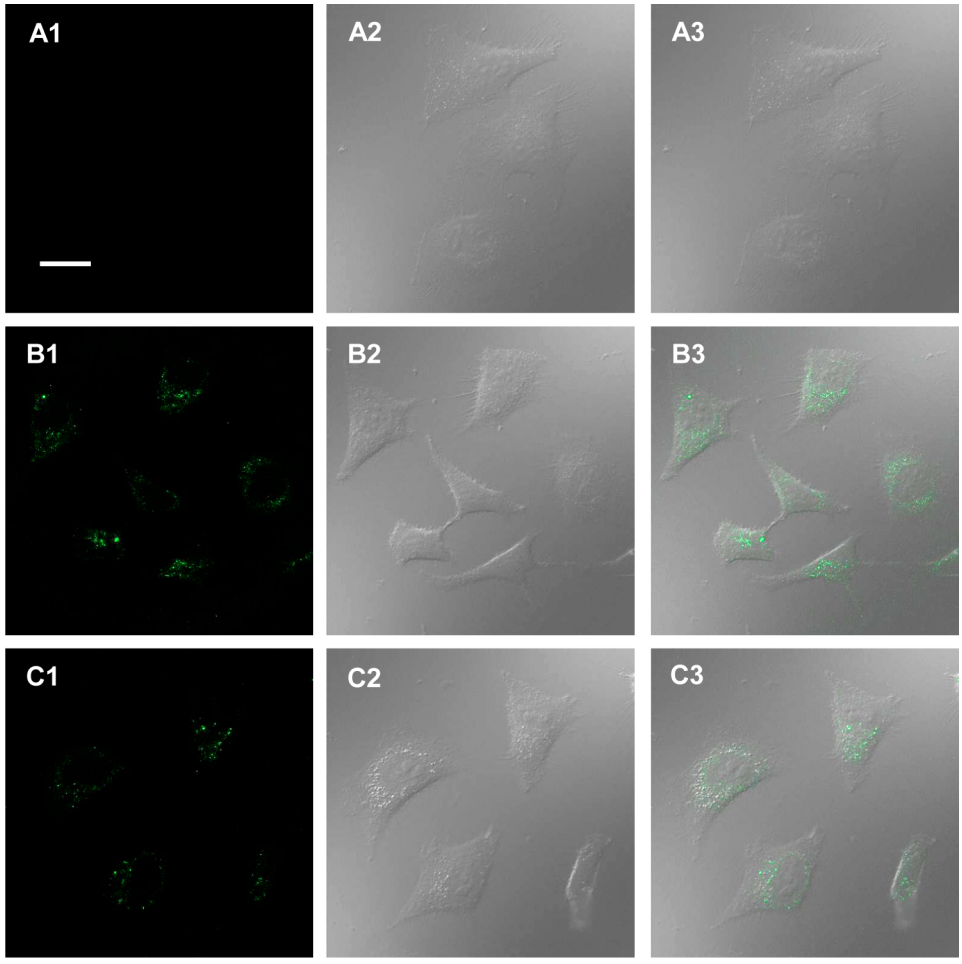

Figure 6. Cofocal fluorescent images of HeLa cells in PBS (pH 7.4) under different conditions: (A1−A3) intact cells; (B1−B3) the treated cells with 100 μg mL^{-1} Dopa-CQD conjugate; (C1−C3) pretreated cells with 200 μM arbutin and then incubated with 100 μg mL^{-1} Dopa-CQD conjugate. Number 1, 2, and 3 represent bright field, fluorescence, and overlap field, respectively. Scale bar, 20 μm.

It is well-known that two intrinsic redox properties of dopamine are normally characterized: a Nernstian dependence of formal potential on pH and oxidation of hydroquinone to quinone by molecular oxygen at basic pH. It has also been reported that QDs-dopamine assemblies show the pH dependent quenching of photoluminescence, and can function as charge transfer coupled pH sensors.[34,35] According to these preceding reports, we speculated that a Dopa-CQDs conjugate would possess a similar pH dependent quenching characteristic induced by similar redox reactions on dopamine. Thus, we first investigated the influence of pH on the fluorescence of Dopa-CQDs in open air, and found that variation of pH values brought a significant impact to its fluorescence. As shown in Figure 2B, the fluorescence of Dopa-CQDs was largely quenched when the pH was over 9.0, and the curve shape of fluorescence emission was also heavily distorted possibly owing to destruction of Dopa-CQDs conjugates under a strong acidic environment. Fluorescence quenching of Dopa-CQDs dependence on pH was exhibited over the pH range 5.1−12.8, consistent with the pH dependent PL quenching phenomenon of QDs-dopamine conjugates.[35] A little difference is that the fluorescence emission spectra of Dopa-CQDs was distorted over pH 11.1 whereas no distortion in emission curve shape was observed for QDs-dopamine conjugate. This distortion in fluorescence emission can be attributed to partial deprotonation of extra carboxyl groups on the surface of carbon quantum dots in Dopa-CQDs. An advantage for pH dependence for Dopa-CQDs is that complete quenching of the fluorescence can be readily achieved over pH 12.8, which offers the feasibility to construct a pH sensor over a wide range from 5.1 to 12.8. Since no apparent distortion in fluorescence can be observed in the pH range 5.1−9.0, the following investigation on its stability was focused on this pH range. The stability of Dopa-CQDs in fluorescence at different pH 5.1, 6.3, and 9.0 was further assessed in open air. Results in Figure S3 indicated that fluorescence intensity of Dopa-CQDs at pH 5.1 and 6.3 almost remains identical within 3 h, but an appreciable decrease in fluorescence for Dopa-CQDs at pH 9.0 was observed, demonstrating that Dopa-CQDs in open air over the pH range 5.1−6.3 is stable in a short period.

Assessment of Detection Strategy for TYR Activity Based on Dopa-CQDs Conjugate. Because it is known that TYR can catalytically oxidize dopamine in the presence of molecular oxygen to quinone derivatives which function as an efficient electron acceptor to quench the fluorescence of its neighboring fluorophores,[36−41] we speculated that as-designed Dopa-CQDs conjugate could be used to assay TYR activity through catalytic oxidization of dopamine moiety and following photoinduced electron transfer. We first evaluated the feasibility of Dopa-CQDs conjugate as a fluorescent conjugate for TYR activity assessment. From Figure 3A, strong fluorescence of Dopa-CQDs conjugate in PB buffer (pH 6.3) in the open air can be recorded; however, almost complete quenching of the

DOI: 10.1021/acsami.5b06711
ACS Appl. Mater. Interfaces 2015, 7, 23564−23574

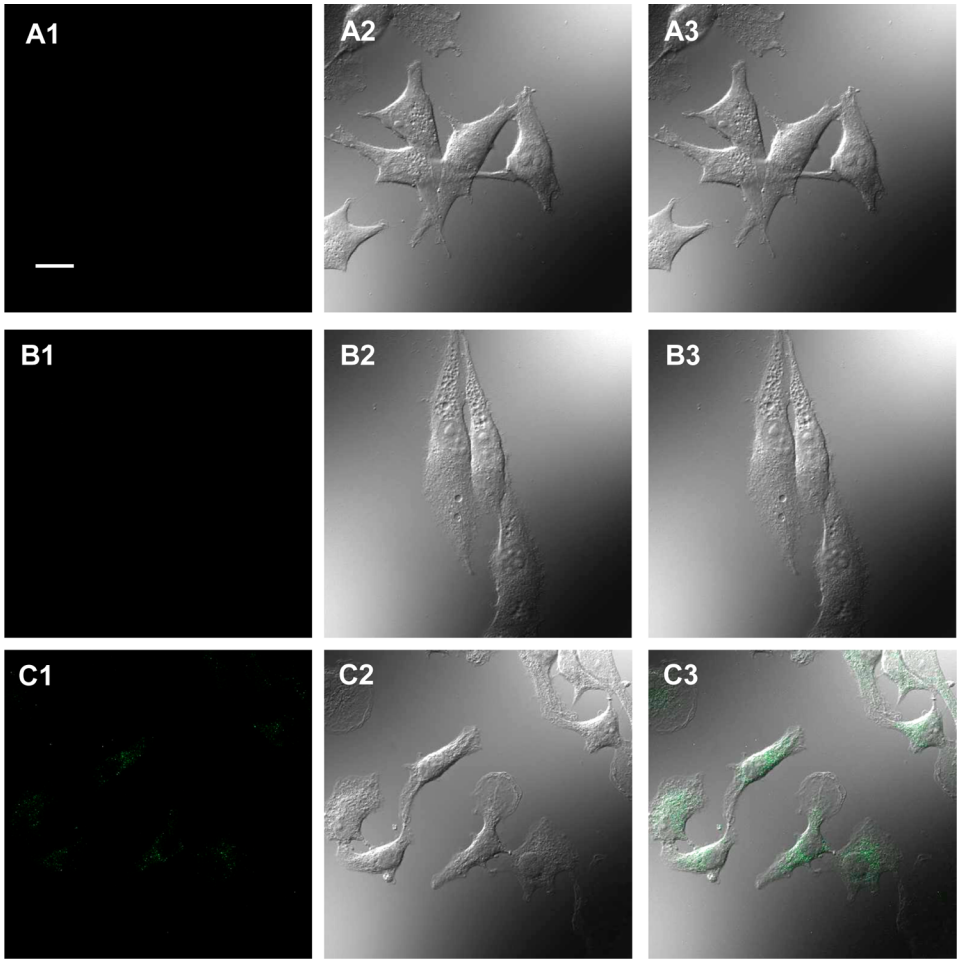

Figure 7. Cofocal fluorescent images of B16 cells in PBS (pH 7.4) under different conditions: (A1−A3) intact cells; (B1−B3) the treated cells with 100 μg mL^{-1} Dopa-CQD conjugate; (C1−C3) pretreated cells with 200 μM arbutin and then incubated with 100 μg mL^{-1} Dopa-CQD conjugate. Number 1, 2, and 3 represent bright field, fluorescence, and overlap field, respectively. Scale bar, 20 μm.

fluorescence was observed after the introduction of 14355.2 U/L of TYR into the preceding conjugate solution within 20 min of incubation time. This observation supported the assumption of quantitative determination of TYR activity using Dopa-CQDs conjugate. Moreover, we further tested its feasibility to function as an inhibitor screening approach by employment of arbutin as an example because arbutin is a well-known inhibitor to TYR.[42−44] A certain amount of arbutin (1666.7 μM) mixed with the same level of TYR to the preceding procedure was incubated for 10 min, and then added into Dopa-CQDs solution. After 20 min of incubation time, the fluorescence of the resultant mixture was recorded as displayed in Figure 3A. In a comparison to that without arbutin, the fluorescence with arbutin was decreased to a very small extent of only about 5%, suggesting that TYR activity was substantially inhibited by the added arbutin. Thus, it is reasonable to assume that Dopa-CQDs conjugate could be exploited to quantify TYR activity in the real-time manner, and designed for screening inhibitors of TYR.

Effective quenching of the fluorescence of Dopa-CQDs conjugate by TYR was observed, which inspired us to explore its underlying mechanism. Previous reports on QDs-Tyr conjugate have provided some clues, where semiconductor quantum dots (QDs) were conjugated with tyrosine to detect TYR activity by means of catalytic oxidation of tyrosine to o-quinone derivative and electron transfer between QDs and generated o-dopaquinone.[16,17] Photoinduced electron transfer (PET) was used to advantage to achieve fluorescence quenching of QDs-Tyr conjugates in the two cases since it has been proven that QDs could be regarded as good electron donors and o-quinone derivatives are good electron acceptors. Quinone derivatives including benzoquinone and naphthoquinone have also been adopted as effective quenchers due to their electron deficiency to quench the fluorescence of AgNCs, and an electron transfer quenching mechanism was supported.[18] Thus, it is assumed that photoinduced electron transfer between CQDs and o-dopaquinone moiety produced by catalytic oxidation of TYR in Dopa-CQDs mainly contributed to fluorescence quenching. To further support this assumption, we first oxidized dopamine moiety in Dopa-CQDs in the presence of TYR (4616.8 U/L) within half an hour, and then inactivated the added TYR for 60 min of heating at 85 °C, and finally added an adequate amount of sodium dithionite into the resulting mixture, where the fluorescence change was monitored as shown in Figure 3B. The presence of TYR in a period of half an hour led to an appreciable reduction in fluorescence intensity of Dopa-CQDs, and the fluorescence intensity was decreased to 40% of the original value. No apparent change in fluorescence was further observed after the treatment of heating, implying that TYR in the solution was inactivated. In the last step, a certain amount of sodium dithionite (333.3 μM), which is a well-known reductant and can reduce quinone to phenol, was added into the preceding mixture. It is found that the majority of the fluorescence was

DOI: 10.1021/acsami.5b06711
ACS Appl. Mater. Interfaces 2015, 7, 23564−23574

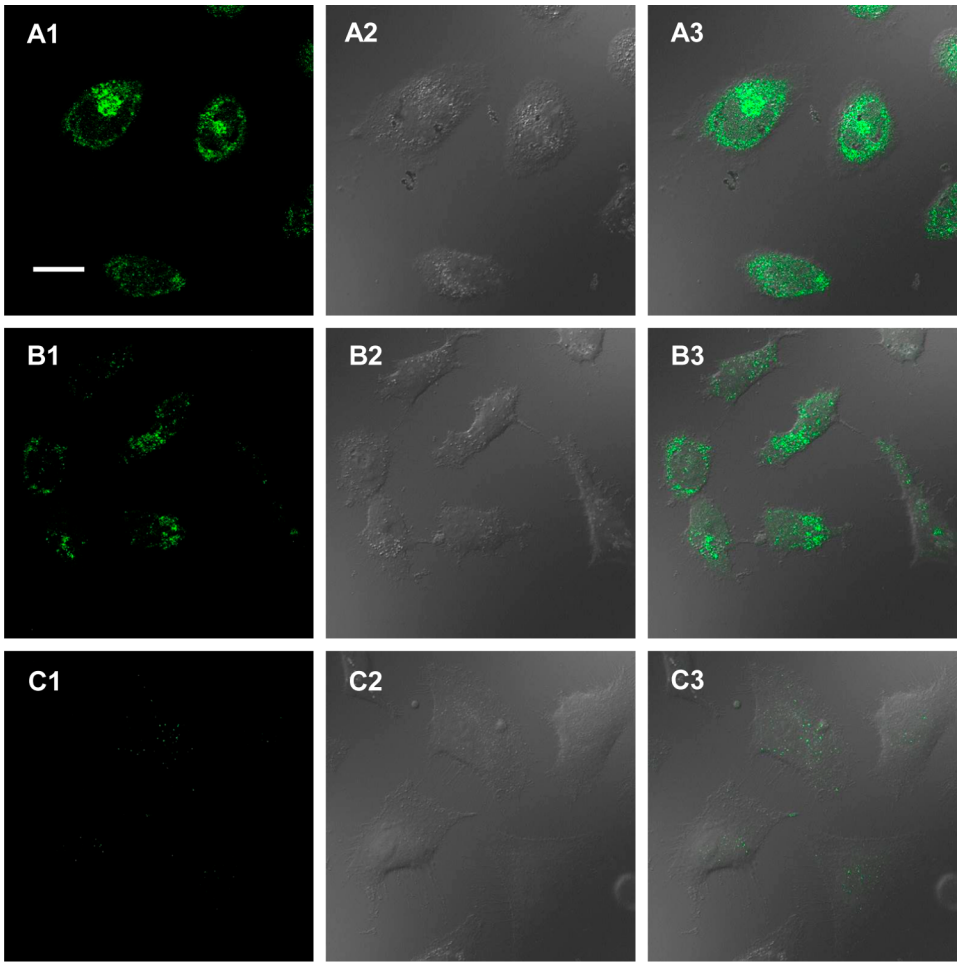

Figure 8. Intracellular pH calibration of Dopa-CQD in HeLa cells. The cells were incubated with 100 μg mL^{-1} Dopa-CQD, and the images were clamped at pH 5.8 (A1−A3), 7.4 (B1−B3), and 9.0 (C1−C3), respectively. Scale bar, 20 μm.

recovered after the introduction of sodium dithionite, during which the o-dopaquinone derivative was reduced to its reductive form such as dopamine. This appreciable fluorescence enhancement by reduction reaction provides a piece of evidence for photoinduced electron transfer quenching mechanism. The former fluorescence quenching can be attributed to PET process between CQDs and o-dopaquinone moiety in the conjugate; however, the specific PET process was blocked after o-dopaquinone was reduced to dopamine derivative by sodium dithionite because generated dopamine derivative is an electron donor rather than an electron acceptor. Apart from substantial fluorescence recovery in intensity, an apparent blue-shift in fluorescence emission peak for oxidative product of Dopa-CQDs was also observed, but no appreciable change in fluorescence of original Dopa-CQDs was found under the same reduction treatment. It has been reported that catalytic oxidation of dopamine by TYR is followed by simultaneous cyclization reaction where dopachrome derivatives formed. Moreover, the transformation of dopamine moiety to dopaquinone in Dopa-CQDs conjugate was also monitored using UV−vis spectroscopy. The apparent difference in absorption spectra between them shown in Figure S4 provided another piece of evidence for this transformation process, which is similar to the finding in QD-Tyr conjugate.[17] In this sense, it is reasonable to assume that this blue-shift in fluorescence probably originated from the formation of dopachrome moiety generated from oxidation and following cyclization reaction. Therefore, it is supported that photoinduced electron transfer inside Dopa-CQDs conjugate is responsible for its fluorescence quenching. PET process takes place inside Dopa-CQDs; i.e, the electron donor and electron acceptor are bonded to each other, different from QDs-Tyr conjugates which are assembled in a noncovalent manner. Thus, the specific PET process occurring in Dopa-CQDs can be expressed as intraparticle PET to differ from the others in terms of intramolecular PET because electron donor and electron acceptor are covalently linked in one nanoparticle.

Real-Time Fluorescent Assay for TYR Activity. By means of catalytic oxidation of dopamine moiety in Dopa-CQDs to dopaquinone by TYR and the following intraparticle PET process, TYR level can be related to the quenching efficiency of the fluorescence. According to the preceding investigation on stability of Dopa-CQDs conjuage at variable pHs, Dopa-CQDs conjugate remains stable over pH range 5.1−9.0 in a period of half an hour. In addition, it is reported that the optimum pH condition for tyrosinase activity is at pH 6−7.[45,46] The optimum conditions for enzymatic process of TYR including pH and reaction time were further explored, and the results in Figure S5 showed that the enzymatic efficiency $(I_0 - I)/t$, where I_0, I, and t represent the original fluorescence intensity of Dopa-CQDs, fluorescence intensity after the addition of TYR, and enzymatic reaction time, increased as the function of pH value ranging from 3.9 to 6.3, demonstrating that the enzymatic reaction occurred in

DOI: 10.1021/acsami.5b06711
ACS Appl. Mater. Interfaces 2015, 7, 23564−23574

the most efficient manner at pH 6.3. Hence, phosphate buffer solution (pH 6.3) was adapted as the standard buffer in the following detection. Under this condition the fluorescence changes of Dopa-CQDs conjugate upon addition of tyrosinase were monitored at a fixed time interval of 1.5 min over a period of 13.5 min. As seen from Figure 4A, the emission of Dopa-CQDs conjugate is gradually quenched after the addition of 7213.3 U/L of TYR to the solution in a period of 9 min, and no apparent change in fluorescence was observed over 9 min. During this process, dopamine moiety in Dopa-CQDs was first specifically oxidized by added TYR to o-dopaquinone derivative which acts as an efficient quencher to CQDs moiety. Then, progressive fluorescence quenching due to intraparticle PET occurred as stepwise oxidation of dopamine moiety is carried on within 9 min of reaction time. After that, almost unchangeable fluorescence was recorded, indicating that the equilibrium of the oxidation reaction was attained. Compared with those based on organic molecules reported previously (32−40 min),[12,13] the equilibrium time is much shorter because it is reported that oxidation rate of diphenol to o-quinones is much faster than that of hydroxylation of monophenol to diphenol.[1] Moreover, we further investigated fluorescence quenching dependent on reaction time when a high level of TYR was used and a large quenching efficiency could be attained. As shown in Figure S6, a much higher level of TYR (15389.3 U/L) was added into Dopa-CQDs solution, and a larger fluorescence quenching efficiency of up to 70% could be reached and remained within a short period of 20 min. Thus, the duration of 20 min was chosen as the optimum reaction time for catalytic oxidation of Dopa-CQDs by TYR.

Under the optimum conditions, quantitative detection of TYR activity was carried out by monitoring the fluorescence of Dopa-CQDs in the presence of a varying amount of TYR. PB buffer solution of Dopa-CQDs (3.0 mL) was mixed with a series of TYR solutions with different levels from 0.0 to 14 355.2 U/L, and then the fluorescence of the resulting mixture was recorded after 20 min of incubation time. Figure 4B illustrated that the fluorescence of Dopa-CQDs conjugate was progressively decreased as the TYR level is rising, and the majority of the fluorescence was almost completely quenched when TYR level is up to 14 355.2 U/L, indicating that most dopamine moieties of the conjugates were catalytically oxidized to dopaquinone derivatives. Figure 4C showed the declining trend in fluorescence intensity of Dopa-CQDs conjugate as a function of TYR activity, and an excellent linear relationship between fluorescence intensity and TYR activity in the range from 23.2 to 793.5 U/L was established as displayed in Figure 4C inset, where the regression equation can be expressed as $y = -0.245x + 872.89$ with $R^2 = 0.99$. The detection limit for TYR activity based on three standard errors was calculated to be 7.0 U/L, which is comparable to or slightly better than those based on AuNPs (6 U/L)[19] and organic molecules (10−20 U/L).[13,14] The selectivity test of the assay toward TYR was conducted as follows: eight potentially interfering substances including glucose oxidase (GOx), DNA, bovine serum albumin (BSA), immunoglobulin G (IgG), alkaline phosphatase (ALP), acid phosphatase (ACP), acetylcholinesterase (AChE), and tyrosinase (TYR) with the same concentration were separately added into Dopa-CQDs assay solution, and then the fluorescence was monitored. As shown in Figure 4D, no apparent response in fluorescence intensity was observed when a given amount of GOx, DNA, BSA, IgG, ALP, ACP, or AChE was present in the solution; however, a sharp decline in fluorescence intensity was recorded when the same amount of TYR to the others was added in the assay solution. The quenching efficiency for TYR was up to nearly 10 while the value of I_0/I for the others was around 1 as the blank, indicating the excellent selectivity of our assay toward TYR.

Inhibitor Screening for TYR. As described in the preceding part, the presence of inhibitor could block the PET process and then further reduce or stop the quenching of the fluorescence, which could be utilized to screen TYR inhibitors. Arbutin, as a well-known TYR inhibitor, was taken as the example to test the screening function of this assay. As shown in Figure 5, the fluorescence of Dopa-CQDs conjugate was quenched by 60% in the presence of tyrosinase without arbutin within 22.5 min, but the addition of 133.3 μM arbutin caused only about 40% of fluorescence quenching under the same conditions. Progressive increase of the concentration of arbutin from 133.3 to 1666.7 μM leads to stepwise decrease of fluorescence quenching from 40% to almost zero, and no apparent fluorescence quenching can be observed when the concentration of added arbutin is over 1000.1 μM, which provides solid evidence that arbutin is an effective inhibitor for tyrosinase activity. It can be concluded from the preceding results that Dopa-CQDs conjugate can be designed for tyrosinase activity analysis and the screening of potential inhibitors.

Cytotoxcity Test and Intracellular Sensing. Successful establishment of fluorometric real-time assay for TYR activity in vitro encouraged us to detect TYR activity in living cells. It is reported that high TYR level is present in B16 melanoma cells while HeLa cells show low TYR expression,[47] and thus B16 melanoma cells and HeLa cells were chosen as the experimental model and negative control, respectively. Cytotoxicity of Dopa-CQDs conjugate to HeLa cells was first assessed using MTT standard assay. The results on cytotoxicity assessment shown in Figure S7 indicated that the Dopa-CQD conjugate possesses very low toxicity to human HeLa cells because total cell viability of tested cells remains at the high level even when the concentration of Dopa-CQD conjugate is up to 240 μg mL^{-1}. Compared to the cytotoxicity test of mere CQDs in our previous report that high cell viability was attained when the concentration of CQDs is less than 100 μg mL^{-1},[48] as-prepared Dopa-CQDs conjugate exhibits much lower cytotoxicity to human HeLa cells, indicating its excellent biocompatibility. The confocal fluorescence images of HeLa and B16 cells were acquired after incubation by 100 μg mL^{-1} Dopa-CQDs conjugate for 5 h, respectively. As shown in Figure 6, HeLa cells show bright fluorescence signals without quenching after incubation with Dopa-CQDs conjugate, and no appreciable fluorescence enhancement can be observed for HeLa cells after pretreatment with 200 μM arbutin, demonstrating the low tyrosinase expression level in HeLa cells, which is consistent with the observation based on QD-Tyr conjugates.[17] However, almost no fluorescence signal was observed in B16 cells after incubation with the same amount of Dopa-CQDs conjugate to that in HeLa cells (Figure 7), indicating that tyrosinase with a high level in B16 cells catalytically oxidized dopamine moiety in the conjugate to o-dopaquinone and thus caused a significant fluorescence quenching of the conjugate. In order to further verify whether fluorescence quenching originated from catalytic oxidation of Dopa-CQDs conjugate by TYR inside B16 cells, TYR inhibition experiments were conducted by pretreating B16 cells with arbutin, which has been proven to be an effective inhibitor in the inhibitor screening part. According to the preceding results, 200 μM of arbutin was used to treat B16 cells before the conjugate. Figure 7 clearly shows that a bright fluorescence signal was observed for pretreated B16 cells with arbutin in comparison

DOI: 10.1021/acsami.5b06711
ACS Appl. Mater. Interfaces 2015, 7, 23564−23574

with unobservable fluorescence without arbutin, indicating that the presence of TYR inside B16 cells results in PL quenching of the conjugate, and arbutin could efficiently inhibit the oxidation ability of TYR inside cells. These positive results illustrated that Dopa-CQD conjugate could be potentially used to monitor tyrosinase expression level in melanocytes and assist the treatment of tyrosinate-associated diseases.

To demonstrate the practicability of Dopa-CQDs conjugate to quantifying intracellular pH, the intracellular calibration experiment was first made in HeLa cells with H^+/K^+ ionophore nigericin, which is a standard approach for homogenizing the pH of cells and culture medium.[49] As shown in Figure 8, bright fluorescence can be recorded from the cells cultured at pH 5.8, and the fluorescence signal was weakened at pH 7.4 in comparison with that at pH 5.8. When the pH was changed to 9.0, only a very faint fluorescence signal can be collected. The fact that the fluorescence from the channel (green pseudocolor) in cells progressively decreases as pH value varies from 5.8 to 9.0 is consistent with the preceding observation in vitro that the fluorescence of the conjugate was dependent on pH in the range 5.0−12.8. The Dopa-CQDs conjugate provided an estimate of intracellular pH increase in cells, and potentially could be used to probe pH change inside cells in a real-time manner.

CONCLUSION

In summary, dopamine functionalized carbon quantum dot (Dopa-CQDs) conjugates were prepared and utilized to design an efficient real-time fluorometric assay for highly sensitive detection of tyrosinase (TYR) activity/level and its inhibitor screening. Carbon quantum dots with strong yellowish green fluorescence were used as the fluorophore, and dopamine with redox property was functionalized on the surface of carbon quantum dots to construct Dopa-CQDs conjugate. Intraparticle photoinduced electron transfer (PET) from CQDs to the dopaquinone moiety in oxidative form of Dopa-CQDs conjugate and specific catalytic oxidation performance of TYR, which could transform dopamine moiety in Dopa-CQDs to dopaquinone derivative in the presence of molecular oxygen, were used to advantage in order to construct the real-time assay for TYR activity. On the basis of this effective PET process, the fluorescence switch-off takes place, and quantitative evaluation of TYR activity was established in terms of the relationship between fluorescence signal readout and present TYR activity. The assay showed good stability and reproducibility by varying the amount of TYR in the assay, and covered a broad linear range of up to 800 U/L with a low detection limit of 7.0 U/L. In addition, a typical inhibitor of TYR arbutin was chosen as an example to assess its function of inhibitor screening, and positive results suggest its potential application for TYR inhibitor screening in the medical and cosmetic industries. Meanwhile, this conjugate was also applied in the intracellular TYR activity detection, and results showed that Dopa-CQDs conjugate possesses high sensitivity and selectivity toward TYR by comparison in fluorescence signal between HeLa and B16 cells, which promises great potential in tyrosinase-associated disease monitoring and medical diagnostics.

ASSOCIATED CONTENT

Supporting Information

The Supporting Information is available free of charge on the ACS Publications website at DOI: 10.1021/acsami.5b06711.

Additional characterization and experimental details (PDF)

AUTHOR INFORMATION

Corresponding Author

*E-mail: qianzhaosheng@zjnu.cn. Phone: +86-579-82282269. Fax: +86-579-82282269.

Author Contributions

L.C. and J.Z. contributed to this work equally.

Notes

The authors declare no competing financial interest.

ACKNOWLEDGMENTS

We are thankful for the support by the National Natural Science Foundation of China (No. 21405142, 21005073, and 21275131) and Zhejiang Province (No. LY13B050001 and LQ13B050002).

REFERENCES

(1) Seo, S.-Y.; Sharma, V. K.; Sharma, N. Mushroom Tyrosinase: Recent Prospects. *J. Agric. Food Chem.* **2003**, *51*, 2837−2853.

(2) Lin, J. Y.; Fisher, D. E. Melanocyte Biology and Skin Pigmentation. *Nature* **2007**, *445*, 843−850.

(3) Slominski, A.; Tobin, D. J.; Shibahara, S.; Wortsman, J. Melanin Pigmentation in Mammalian Skin and Its Hormonal Regulation. *Physiol. Rev.* **2004**, *84*, 1155−1228.

(4) Angeletti, C.; Khomitch, V.; Halaban, R.; Rimm, D. L. Novel Tryamide-Based Tyrosinase Assay for the Detection of Melanoma Cells in Cytological Preparations. *Diagn. Cytopathol.* **2004**, *31*, 33−37.

(5) Baharav, E.; Merimski, O.; Shoenfeld, Y.; Zigelman, R.; Gilbrud, B.; Yecheskel, G.; Youinou, P.; Fishman, P. Tyrosinase As an Autoantigen in Patients with Vitiligo. *Clin. Exp. Immunol.* **1996**, *105*, 84−88.

(6) Friedman, M. Food Browning and Its Prevention: an Overview. *J. Agric. Food Chem.* **1996**, *44*, 631−653.

(7) Boyer, R. F. Spectrophotometric Assay of Polyphenoloxidase Activity. A special Project in Enzyme Characterization. *J. Chem. Educ.* **1977**, *54*, 585−586.

(8) Park, Y.-D.; Lee, J.-R.; Park, K.-H.; Hahn, H.-S.; Hahn, M.-J.; Yang, J.-M. A New Continuous Spectrophotometric Assay Method for DOPA Oxidase Activity of Tyrosinase. *J. Protein Chem.* **2003**, *22*, 473−480.

(9) Kong, F. J.; Liu, H. F.; Dong, J.; Qian, W. P. Growth-Sensitive Gold Nanoshells Precursor Nanocomposites for the Detection of L-DOPA and Tyrosinase Activity. *Biosens. Bioelectron.* **2011**, *26*, 1902−1907.

(10) Li, S.; Mao, L. Y.; Tian, Y. P.; Wang, J.; Zhou, N. D. Spectrophotometric Detection of Tyrosinase Activity Based on Boronic Acid-Functionalized Gold Nanoparticles. *Analyst* **2012**, *137*, 823−825.

(11) Yildiz, H. B.; Freeman, R.; Gill, R.; Willner, I. Electrochemcial, Photoelctrochemical, and Piezoelectric Analysis of Tyrosinase Activity by Functionalized Nanoparticles. *Anal. Chem.* **2008**, *80*, 2811−2816.

(12) Feng, X. L.; Feng, F. D.; Yu, M. H.; He, F.; Xu, Q. L.; Tang, H. W.; Wang, S.; Li, Y. L.; Zhu, D. B. Synthesis of a New Water-Soluble Oligo(phenylenevinylenen) Containing a Tyrosine Moiety for Tyrosinase Activity Detection. *Org. Lett.* **2008**, *10*, 5369−5372.

(13) Li, X. H.; Shi, W.; Chen, S. M.; Jia, J.; Ma, H. M.; Wolfbeis, O. S. A Near-infrared Fluorescent Probe for Monitoring Tyrosinase Activity. *Chem. Commun.* **2010**, *46*, 2560−2562.

(14) Yan, S. Y.; Huang, R.; Wang, C. C.; Zhou, Y. M.; Wang, J. Q.; Fu, B. S.; Weng, X. C.; Zhou, X. A Two-photon Fluorescent Probe for Intracellular Detection of Tyrosinase Activity. *Chem. - Asian J.* **2012**, *7*, 2782−2785.

(15) Wang, C. C.; Yan, S. Y.; Huang, R.; Feng, S.; Fu, B. S.; Weng, X. C.; Zhou, X. A Turn-on Fluorescent Probe for Detection of Tyrosinase Activity. *Analyst* **2013**, *138*, 2825−2828.

(16) Gill, R.; Freeman, R.; Xu, J.-P.; Willner, I.; Winograd, S.; Shweky, I.; Banin, U. Probing Biocatalytic Transfromations with CdSe-ZnS QDs. *J. Am. Chem. Soc.* **2006**, *128*, 15376−15377.

DOI: 10.1021/acsami.5b06711
ACS Appl. Mater. Interfaces 2015, 7, 23564−23574

(17) Zhu, X. L.; Hu, J.; Zhao, Z. H.; Sun, M. J.; Chi, X. Q.; Wang, X. M.; Gao, J. H. Kinetic and Sensitivie Analysis of Tyrosinase Activity Using Electron Transfer Complexes: in Vitro and Intracellular Study. *Small* **2015**, *11*, 862−879.
(18) Liu, X. Q.; Wang, F. A.; Niazov-Elkan, A.; Guo, W. W.; Willner, I. Probing Biocatalytic Transformations with Luminescent DNA/Silver Nanoclusters. *Nano Lett.* **2013**, *13*, 309−314.
(19) Teng, Y.; Jia, X. F.; Li, J.; Wang, E. K. Ratiometric Fluorescence Detection of Tyrosinase Activity and Dopamine Using Thiolate-protected Gold Nanoclusters. *Anal. Chem.* **2015**, *87*, 4897−4902.
(20) Baker, S. N.; Baker, G. A. Luminescent Carbon Nanodots: Emergent Nanolights. *Angew. Chem., Int. Ed.* **2010**, *49*, 6726−6744.
(21) Shen, J. H.; Zhu, Y. H.; Yang, X. L.; Li, C. Z. Graphene Qauntum Dots: Emergent Nanolighs for Bioimaging, Sensors, Catalysis and Photovoltaic Devices. *Chem. Commun.* **2012**, *48*, 3686−3699.
(22) Zhao, A. D.; Chen, Z. W.; Zhao, C. Q.; Gao, N.; Ren, J. S.; Qu, X. G. Recent Advances in Bioapplications of C-dots. *Carbon* **2015**, *85*, 309−327.
(23) Zheng, X. T.; Ananthanarayanan, A.; Luo, K. Q.; Chen, P. Glowing Graphene Quantum Dots and Carbon Dots: Properties, Syntheses, and Biological Applications. *Small* **2015**, *11*, 1620−1636.
(24) Lim, S. Y.; Shen, W.; Gao, Z. Q. Carbon Quantum Dots and Their Applications. *Chem. Soc. Rev.* **2015**, *44*, 362−381.
(25) Qian, Z. S.; Shan, X. Y.; Chai, L. J.; Ma, J. J.; Chen, J. R.; Feng, H. A Universal Fluorescence Sensing Strategy Based on Biocompatible Graphene Quantum Dots and Graphen Oxide for the Detection of DNA. *Nanoscale* **2014**, *6*, 5671−5674.
(26) Qian, Z. S.; Shan, X. Y.; Chai, L. J.; Ma, J. J.; Chen, J. R.; Feng, H. DNA Nanosensor Based on Biocompatible Graphene Quantum Dots and Carbon Nanotubes. *Biosens. Bioelectron.* **2014**, *60*, 64−70.
(27) Qian, Z. S.; Shan, X. Y.; Chai, L. J.; Chen, J. R.; Feng, H. Simultaneous Detection of Multiple DNA Targets by Integrating Dual-color Graphene Quantum Dots Nanoprobes and Carbon Nanotubes. *Chem. - Eur. J.* **2014**, *20*, 16065−16069.
(28) Noh, E.-H.; Ko, H. Y.; Lee, C. H.; Jeong, M.-S.; Chang, Y. W.; Kim, S. Carbon Nanodot-Based Self-delivering MicorRNA Sensor to Visualize MicroRNA124a Expression During Neurogenesis. *J. Mater. Chem. B* **2013**, *1*, 4438−4445.
(29) Li, X.; Zhu, S. J.; Xu, B.; Ma, K.; Zhang, J. H.; Yang, B.; Tian, W. J. Self-assembled Graphene Quantum Dots Induced by Cytochrome c: A Novel Biosensor for Trypsin with Remarkable Fluorescence Enhancement. *Nanoscale* **2013**, *5*, 7776−7779.
(30) Qian, Z. S.; Shan, X. Y.; Chai, L. J.; Chen, J. R.; Feng, H. Dual-colored Graphene Quantum Dots-labeled Nanoprobes/graphene oxide: Functional Carbon Materials for Respective and Simultaneous Detection of DNA and Thrombin. *Nanotechnology* **2014**, *25*, 415501.
(31) Liu, S. Y.; Zhao, N.; Cheng, Z.; Liu, H. G. Amino-functionalized Green Fluorescent Carbon Dots as Surface Energy Transfer Biosensors for Hyaluronidase. *Nanoscale* **2015**, *7*, 6836−6842.
(32) Qian, Z. S.; Chai, L. J.; Huang, Y. Y.; Tang, C.; Shen, J. J.; Chen, J. R.; Feng, H. A Real-time Fluorescent Assay for the Detection of Alkaline Phosphatase Activity Based on Carbon Quantum Dots. *Biosens. Bioelectron.* **2015**, *68*, 675−680.
(33) Qian, Z. S.; Chai, L. J.; Tang, C.; Huang, Y. Y.; Chen, J. R.; Feng, H. Carbon Quantum Dots-based Recyclabe Real-time Fluorescence Assay for Alkaline Phosphatase with Adenosine Triphosphate as Substrate. *Anal. Chem.* **2015**, *87*, 2966−2973.
(34) Medintz, I. L.; Stewart, M. H.; Trammell, S. A.; Susumu, K.; Delehanty, J. B.; Mei, B. C.; Melinger, J. S.; Blanco-Canosa, J. B.; Dawson, P. E.; Mattoussi, H. Quantum-dot/dopamine Bioconjugates Function as Redox Coupled Assemblies for in Vitro and Intracellular pH Sensing. *Nat. Mater.* **2010**, *9*, 676−684.
(35) Ji, X.; Palui, G.; Avellini, T.; Na, H. B.; Yi, C. Y.; Knappenberger, K. L., Jr.; Mattoussi, H. On the pH-dependent Quenching of Quantum Dot Photoluminescence by Redox Active Dopamine. *J. Am. Chem. Soc.* **2012**, *134*, 6006−6017.
(36) Ma, W.; Liu, H.-T.; Long, Y.-T. Monitoring Dopamine Quinone-induced Dopaminergic Neurotoxicity Using Dopamine Functionalized Quantum Dots. *ACS Appl. Mater. Interfaces* **2015**, *7*, 14352−14358.
(37) Ma, W.; Liu, H.-T.; He, X.-P.; Zang, Y.; Li, J.; Chen, G.-R.; Tian, H.; Long, Y.-T. Target-Specific Imaging of Transmembrance Receptors Using Quinonyl Glycosides Functionalized Quantum Dots. *Anal. Chem.* **2014**, *86*, 5502−5507.
(38) Ma, W.; Long, Y.-T. Quinone/Hydroquinone-functionalized Biointerfaces for Biological Applications from Macro- to Nano-scale. *Chem. Soc. Rev.* **2014**, *43*, 30−41.
(39) Ma, W.; Qin, L.-X.; Liu, F.-T.; Gu, Z.; Wang, J.; Pan, Z. G.; James, T. D.; Long, Y.-T. Ubiquinone-quantum Dot Bioconjugates for in Vitro and Intracellular Complex I Sensing. *Sci. Rep.* **2013**, *3*, 1537.
(40) Li, D.-W.; Qin, L.-X.; Li, Y.; Nia, R. P.; Long, Y.-T.; Chen, H.-Y. CdSe/ZnS Quantum dot-cytochrome c Bioconjugates for Selective Intracellular $O_2^{\cdot-}$ Sensing. *Chem. Commun.* **2011**, *47*, 8539−8541.
(41) Qin, L.-X.; Ma, W.; Li, D.-W.; Li, Y.; Chen, X. Y.; Kraatz, H.-B.; James, T. D.; Long, Y.-T. Coenzyme Functionalized CdTe/ZnS Quantum Dots for Reactive Oxygen Species (ROS) Imaging. *Chem. - Eur. J.* **2011**, *17*, 5262−5271.
(42) Funayama, M.; Arakawa, H.; Yamamoto, R.; Nishino, T.; Shin, T.; Murao, S. Effects of α- and β-arbutin on Activity of Tyrosinase from Mushroom and Mouse Melanoma. *Biosci., Biotechnol., Biochem.* **1995**, *59*, 143−144.
(43) Jin, Y. H.; Lee, S. J.; Chung, M. H.; Park, J. H.; Park, Y. I.; Cho, T. H.; Lee, S. K. Aloesin and Arbutin Inhibit Tyrosinase Activity in a Synergistic Manner via a Different Action Mechanism. *Arch. Pharmacal Res.* **1999**, *22*, 232−236.
(44) Sugimoto, K.; Nishimura, T.; Nomura, K.; Sugimoto, K.; Kuriki, T. Syntheses of Arbutin-α-glycosides and a Comparison of Their Inhibitory Effects with Those of α-arbutin and Arbutin on Human Tyrosinase. *Chem. Pharm. Bull.* **2003**, *51*, 798−801.
(45) Gauillard, F.; Richardforget, F.; Nicolas, J. New Spetrophotometric Assay for Polyphenol Oxidase Activity. *Anal. Biochem.* **1993**, *215*, 59−65.
(46) Baron, R.; Zayats, M.; Willner, I. Dopamine-, L-DOPA-, Adrenaline-, and Noradrenaline-induced Growth of Au Nanoparticles: Assays for the Detection of Neurotransmitters and of Tyrosinase Activity. *Anal. Chem.* **2005**, *77*, 1566−1571.
(47) White, R.; Hu, F. Characteristics of Tyrosinase in B16 Melanoma. *J. Invest. Dermatol.* **1977**, *68*, 272−276.
(48) Chai, L. J.; Zhou, J.; Feng, H.; Lin, J. J.; Qian, Z. S. A Reversible Fluorescence Nanoswitch Based Carbon Quantum Dots Nanoassembly for Detection of Pyrophosphate Ion. *Sens. Actuators, B* **2015**, *220*, 138−145.
(49) Tafani, M.; Cohn, J. A.; Karpinich, N. O.; Rothman, R. J.; Russo, M. A.; Farber, J. L. Regulation of Intracellular pH Mediates Bax Activation in HeLa cells Treated with Staurosporine or Tumor Necrosis Factor-α. *J. Biol. Chem.* **2002**, *277*, 49569−49576.

DOI: 10.1021/acsami.5b06711
ACS Appl. Mater. Interfaces 2015, 7, 23564−23574